ICIC Express Letters
Part B: Applications
Volume **14**, Number **2**, February **2023**

ICIC International ©2023 ISSN 2185-2766
pp. **211–218**

A HOVER ATTITUDE CONTROL SYSTEM ON A QUAD TILT WING UNMANNED AERIAL VEHICLE USING LINEAR QUADRATIC REGULATOR METHOD

Ariesta Martiningtyas Handayani, Ahmad Ashari* and Jazi Eko Istiyanto

Department of Computer Science and Electronics
Faculty of Mathematics and Natural Sciences
Universitas Gadjah Mada
Sekip Utara PO BOX BLS 21, Yogyakarta 55281, Indonesia
ariesta_mh@mail.ugm.ac.id; jazi@ugm.ac.id
*Corresponding author: ashari@ugm.ac.id

Received June 2022; accepted September 2022

Abstract. *Quad Tilt Wing Unmanned Aerial Vehicle (QTW UAV) can fly Vertical Take-Off and Landing (VTOL) and also horizontally (Cruise). The QTW UAV can fly near a stationary state during hover. Stationary flying can be done by maintaining the orientation of the Euler angle of the rollers and pitch at 0°, the yaw angle in a particular direction, and the altitude (on the vertical axis of the earth). QTW UAV requires a control system that can maintain a stationary state. The Linear Quadratic Regulator (LQR) method is one of the control systems to maintain a stationary state. This ability is done in order to minimize the error response approaching zero. The LQR method uses the state as feedback to control the attitude of the UAV. The simulation of the QTW UAV model was carried out to obtain the test results of the control system method.*
Keywords: QTW UAV, LQR, Hover, Stationer, Error response

1. **Introduction.** A UAV is a vehicle that can fly autonomously using autopilot or controlled remotely so that no pilot is in the vehicle [1]. Fixed-wing UAV is an unmanned aircraft that can fly using the lift generated by the wing construction and the thrust from the propulsion system [2]. A rotary-wing UAV is an unmanned aircraft with a rotor as propeller [3].

Both fixed-wing and rotary-wing UAVs have several advantages and disadvantages. Fixed-wing UAVs require a long runway for taking off and landing. In contrast, rotary-wing UAVs can perform VTOL [4]. Fixed-wing UAV has a high cruising range. However, rotary-wing UAVs do not fly a long distance [5]. As a result, the rotary-wing UAVs do not have a high cruising range [6-8].

Developing a UAV capable of achieving a long flight range and performing VTOL is still an exciting topic of research. The VTOL plane is one potential solution. The VTOL plane combines the advantages of both the fixed-wing and rotary-wing concepts in one UAV [7,9]. QTW UAV is one type of VTOL plane [10]. QTW UAV combines fixed-wing and rotary-wing concepts in one UAV, thus inheriting the advantages of both [7].

QTW UAV has several flight stages: vertical take-off, hover, transition, cruise, and vertical landing. The transition stage is where the QTW UAV's wings swing to move from hover to cruise and vice versa. The wing swings (tilting) by 90° so that it becomes perpendicular to the previous position [11-13].

However, before going to the transition stage, the QTW UAV must be able to hover close to a stationary state. Altitude and attitude controls are needed for stabilizing the hover flight mode which is a very critical phase of operation since normally airplane does

DOI: 10.24507/icicelb.14.02.211

not perform hover flights [9,14]. As the QTW UAV hover approaches a stationary state, the total force generated by the rotor is equal to the weight of the vehicle under gravity. The direction of the force generated by the rotor is parallel to the direction of the upward vertical force of the vehicle [15,16]. The QTW UAV can fly close to a stationary state by maintaining the orientation of the Euler roll and pitch angles at 0°, the yaw angle in a particular direction, and the altitude (on the vertical axis of the earth). Therefore, a control system is needed to make the QTW UAV fly close to a stationary state.

Several control methods have been implemented on the VTOL plane UAV for various needs, such as Proportional Integral Derivative (PID) [17], adaptive nonlinear hierarchical control [18,19], Linear Quadratic with Integrator (LQI) [6], and LQR [20]. The LQR method uses the state as feedback to control the attitude of the UAV [20]. In this study, LQR is used to maintain the height and slope of the Euler angle to minimize the error response to near zero. A QTW UAV, a type of VTOL plane, is to be supported by LQR to stabilize its hover mode.

The rest of the paper is structured as follows: Section 2 addresses the theory and formulas, Section 3 describes the simulation setup, Section 4 discusses the simulation result, and performance analysis, and finally, Section 5 concludes the paper.

2. Theory and Formulas.

Mathematical models are needed to design methods and algorithms [21]. After the mathematical model is obtained, the LQR method can be simulated on the model. The mathematical model of the QTW UAV is designed based on Newton Euler's concept, which uses Newton's laws and Euler's laws as the basis for transitional and rotational motion. Equations (9), (12), (13), and (14) show mathematical models that reference the dynamics of the QTW UAV.

The inertial frame of the earth is written with the symbol $\mathbf{W}(x_W, y_W, z_W)$ and the inertial frame of the body $\mathbf{B}(x_B, y_B, z_B)$. The position of the Center of Gravity (CoG) in the Earth's inertial frame is written in Equations (1) and (2). Figure 1 shows the inertial frame of the body against the inertial frame of the Earth.

$$\mathbf{P_W} = [X, Y, Z]^T \tag{1}$$

$$\mathbf{V_W} = \dot{\mathbf{P}}_\mathbf{W} = \left[\dot{X}, \dot{Y}, \dot{Z}\right]^T \tag{2}$$

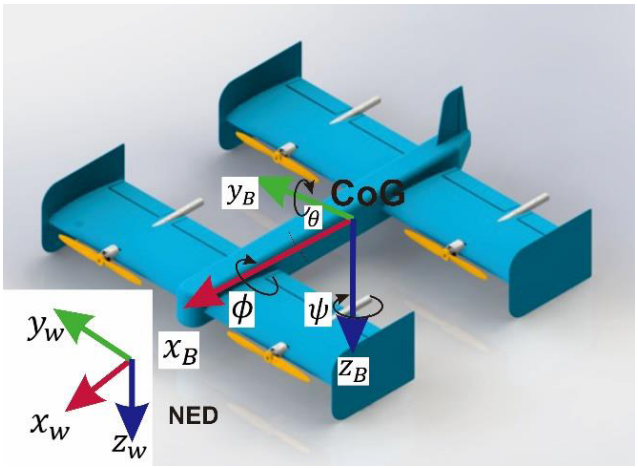

FIGURE 1. Inertial framework of the body against the Earth's inertial framework

QTW UAV has several parameters that reflect the attitude of the vehicle. These parameters include the angles of roll (ϕ), pitch (θ), and yaw (ψ), which are shown in Equation (3), and the rotational speed is shown in Equation (4). The position of the vehicle can be determined using the rotation matrix ${}^{\mathbf{E}}\mathbf{R}_{\mathbf{B}}$. The rotation matrix ${}^{\mathbf{E}}\mathbf{R}_{\mathbf{B}}$ is obtained from

the product of the rotation matrix on the x-axis ($\mathbf{R}_x(\phi)$), the rotation matrix on the y-axis ($\mathbf{R}_y(\theta)$), and the rotation matrix on the z-axis ($\mathbf{R}_z(\psi)$). ${}^{\mathbf{E}}\mathbf{R}_{\mathbf{B}}$ is a rotation matrix that represents the orientation of the body frame to the Earth's frame, which is written in Equation (5), in which c represents cosine, and s represents sine.

$$\boldsymbol{\alpha}_W = [\phi, \theta, \psi]^T \tag{3}$$

$$\boldsymbol{\Omega}_W = \dot{\boldsymbol{\alpha}}_W = \left[\dot{\phi}, \dot{\theta}, \dot{\psi}\right]^T \tag{4}$$

$${}^{\mathbf{E}}\mathbf{R}_{\mathbf{B}}\left(\boldsymbol{\phi}, \boldsymbol{\theta}, \boldsymbol{\psi}\right) = \begin{bmatrix} c\psi c\theta & s\phi s\theta s\psi - c\phi s\psi & -c\phi s\theta c\psi + s\phi s\psi \\ s\psi c\theta & s\phi s\theta s\psi + c\phi c\psi & s\phi s\theta s\psi - s\phi c\psi \\ -s\theta & s\phi c\theta & c\phi c\theta \end{bmatrix} \tag{5}$$

QTW UAV dynamics can be written into Equation (6).

$$\begin{bmatrix} m\mathrm{I}_{3\times3} & 0_{3\times3} \\ 0_{3\times3} & \mathrm{I}_b \end{bmatrix} \begin{bmatrix} \dot{\mathbf{V}}_W \\ \dot{\boldsymbol{\Omega}}_b \end{bmatrix} + \begin{bmatrix} 0 \\ \boldsymbol{\Omega}_b \times (\boldsymbol{I}_b \cdot \boldsymbol{\Omega}_b) \end{bmatrix} = \begin{bmatrix} \boldsymbol{F}_T \\ \boldsymbol{\tau}_T \end{bmatrix} \tag{6}$$

The gain of the force that occurs on each of the translational axes (on the z-axis) is shown in Equation (7).

$$\boldsymbol{F} = {}^{\boldsymbol{E}}\boldsymbol{R}_{\boldsymbol{B}} \cdot \boldsymbol{F}_{\boldsymbol{th}} + \boldsymbol{F}_{\boldsymbol{g}} \tag{7}$$

Newton's second law governs the relationship between the force F and the acceleration experienced by the center of mass. In addition, the gravitational force expressed at NED (North East Down) is shown in Equation (8).

$$F_g = -\begin{bmatrix} 0 \\ 0 \\ mg \end{bmatrix} \tag{8}$$

The equation of translational motion in hover mode QTW UAV can be derived from Newton's second law. The equation is shown in Equation (9).

$$F_z = {}^{E_z}R_{B_z} \cdot F_{th_z} + F_{g_z} \tag{9}$$

$$m \cdot \ddot{Z} = (c\phi c\theta)\, F_z - mg, \;\; \ddot{Z} = \frac{c\phi c\theta}{m} F_z - g$$

Euler's second law explains the relationship between the torque ($\boldsymbol{\tau}$) and the angular velocity ($\boldsymbol{\omega}$) as shown in Equation (10),

$$\boldsymbol{\tau} = (\mathbf{I} \cdot \boldsymbol{\omega}) \times \boldsymbol{\omega} + \mathbf{I} \cdot \dot{\boldsymbol{\omega}} \tag{10}$$

where

$$\boldsymbol{\omega} = \begin{pmatrix} \dot{\phi} & \dot{\theta} & \dot{\psi} \end{pmatrix}^T, \; \mathbf{I} = \begin{bmatrix} I_{xx} & 0 & 0 \\ 0 & I_{yy} & 0 \\ 0 & 0 & I_{zz} \end{bmatrix}$$

I_{xx}, I_{yy}, I_{zz} are the moments of inertia around the body's x, y, and z axes, respectively.

The calculation of the torque around the x-axis of the body (B_x), the y-axis of the body (B_y) and the z-axis of the body (B_z) based on Euler's second law is shown in Equation (11).

$$\begin{bmatrix} I_{xx} & 0 & 0 \\ 0 & I_{yy} & 0 \\ 0 & 0 & I_{zz} \end{bmatrix} \begin{bmatrix} \ddot{\phi} \\ \ddot{\theta} \\ \ddot{\psi} \end{bmatrix} + \begin{bmatrix} \dot{\phi} \\ \dot{\theta} \\ \dot{\psi} \end{bmatrix} \times \left(\begin{bmatrix} I_{xx} & 0 & 0 \\ 0 & I_{yy} & 0 \\ 0 & 0 & I_{zz} \end{bmatrix} \begin{bmatrix} \dot{\phi} \\ \dot{\theta} \\ \dot{\psi} \end{bmatrix} \right) = \begin{bmatrix} \tau_\phi \\ \tau_\theta \\ \tau_\psi \end{bmatrix} \tag{11}$$

$$\begin{bmatrix} I_{xx}\ddot{\phi} \\ I_{yy}\ddot{\theta} \\ I_{zz}\ddot{\psi} \end{bmatrix} + \begin{bmatrix} I_{zz}\dot{\psi}\dot{\theta} - I_{yy}\dot{\psi}\dot{\theta} \\ I_{zz}\dot{\psi}\dot{\phi} - I_{xx}\dot{\psi}\dot{\phi} \\ I_{yy}\dot{\phi}\dot{\theta} - I_{xx}\dot{\phi}\dot{\theta} \end{bmatrix} = \begin{bmatrix} \tau_\phi \\ \tau_\theta \\ \tau_\psi \end{bmatrix}$$

Three equations of torque QTW UAV when running hover mode can be seen in Equations (12), (13), and (14).

1) Torque around the B_x body (ϕ rotation)

$$I_{xx}\ddot{\phi} + (I_{zz} - I_{yy})\,\dot{\psi}\dot{\theta} = \tau_\phi$$
$$\ddot{\phi} = \frac{1}{I_{xx}}\tau_\phi + \frac{(I_{yy} - I_{zz})}{I_{xx}}\dot{\theta}\dot{\psi} \tag{12}$$

2) Torque around the B_y body (θ rotation)

$$I_{yy}\ddot{\theta} + (I_{zz} - I_{xx})\,\dot{\psi}\dot{\phi} = \tau_\theta$$
$$\ddot{\theta} = \frac{1}{I_{yy}}\tau_\theta + \frac{(I_{xx} - I_{zz})}{I_{yy}}\dot{\psi}\dot{\phi} \tag{13}$$

3) Torque around the B_z body (ψ rotation)

$$I_{zz}\ddot{\psi} + (I_{yy} - I_{xx})\,\dot{\phi}\dot{\theta} = \tau_\psi$$
$$\ddot{\psi} = \frac{1}{I_{xx}}\tau_\psi + \frac{(I_{xx} - I_{yy})}{I_{zz}}\dot{\phi}\dot{\theta} \tag{14}$$

Actions generated by the control method consisting of F_z, τ_ϕ, τ_θ, and τ_ψ are aliased to u_1, u_2, u_3, and u_4, respectively as shown in Equations (15), (16), (17), and (18).

$$u_1 = k\left(\omega_1^2 + \omega_2^2 + \omega_3^2 + \omega_4^2\right) \tag{15}$$
$$u_2 = kL_s\left(\omega_1^2 - \omega_2^2 + \omega_3^2 - \omega_4^2\right) \tag{16}$$
$$u_3 = kL_l\left(\omega_1^2 + \omega_2^2 - \omega_3^2 - \omega_4^2\right) \tag{17}$$
$$u_4 = k\lambda\left(\omega_1^2 - \omega_2^2 - \omega_3^2 + \omega_4^2\right) \tag{18}$$

where k is the motor thrust constant, L_s and L_l are the distances from the rotor to CoG along the y and x-axes, respectively, and λ is the torque/force ratio.

3. **Simulation Setup.** The control method used in this study is the LQR. The LQR is a regulator control that aims to bring the system to a predetermined state by setting the error to zero with the minimum cost function value. LQR produces the full-state feedback control system's gain **K** value [2,20].

Based on the model described earlier, the QTW UAV is a MIMO (Multiple Input Multiple Output) system. The state space equation is indicated by Equation (19).

$$\dot{\mathbf{x}} = \mathbf{A}\mathbf{x} + \mathbf{B}\mathbf{u} \tag{19}$$

The state-space equation is obtained from the equations of the previous mathematical model, which consists of two motions namely, the translational and the rotational motion as shown in Equations (10), (13), (14), and (15). These equations are converted into state-space equations, shown in Equation (20).

$$\begin{bmatrix} \dot{Z} \\ \ddot{Z} \\ \dot{\phi} \\ \ddot{\phi} \\ \dot{\theta} \\ \ddot{\theta} \\ \dot{\psi} \\ \ddot{\psi} \end{bmatrix} = \begin{bmatrix} 0 & 1 & 0 & 0 & 0 & 0 & 0 & 0 \\ 0 & 0 & 0 & 0 & 0 & 0 & 0 & 0 \\ 0 & 0 & 0 & 1 & 0 & 0 & 0 & 0 \\ 0 & 0 & 0 & 0 & 0 & \frac{I_{yy} - I_{zz}}{I_{yy}}\dot{\psi} & 0 & 0 \\ 0 & 0 & 0 & 0 & 0 & 1 & 0 & 0 \\ 0 & 0 & 0 & \frac{I_{xx} - I_{zz}}{I_{yy}}\dot{\psi} & 0 & 0 & 0 & 0 \\ 0 & 0 & 0 & 0 & 0 & 0 & 0 & 1 \\ 0 & 0 & 0 & 0 & 0 & \frac{I_{xx} - I_{yy}}{I_{zz}}\dot{\phi} & 0 & 0 \end{bmatrix} \begin{bmatrix} Z \\ \dot{Z} \\ \phi \\ \dot{\phi} \\ \theta \\ \dot{\theta} \\ \psi \\ \dot{\psi} \end{bmatrix} + \begin{bmatrix} 0 & 0 & 0 & 0 \\ \frac{c\phi c\theta}{m} & 0 & 0 & 0 \\ 0 & 0 & 0 & 0 \\ 0 & \frac{1}{I_{xx}} & 0 & 0 \\ 0 & 0 & 0 & 0 \\ 0 & 0 & \frac{1}{I_{yy}} & 0 \\ 0 & 0 & 0 & 0 \\ 0 & 0 & 0 & \frac{1}{I_{zz}} \end{bmatrix} \begin{bmatrix} F_z \\ \tau_\phi \\ \tau_\theta \\ \tau_\psi \end{bmatrix} \tag{20}$$

The block diagram of the control system on the hovering QTW UAV is shown in Figure 2. Based on Figure 2, **u** is the action produced by the control system, which is the product of the gain **K** and the entire state of the controlled system **x**. Action **u** consists of four elements, namely u_1, u_2, u_3, and u_4 as vertical force, roll torque, pitch torque, and yaw torque. **A**, **B**, and **C** are matrix characteristics of the system according to the state space in Equation (20).

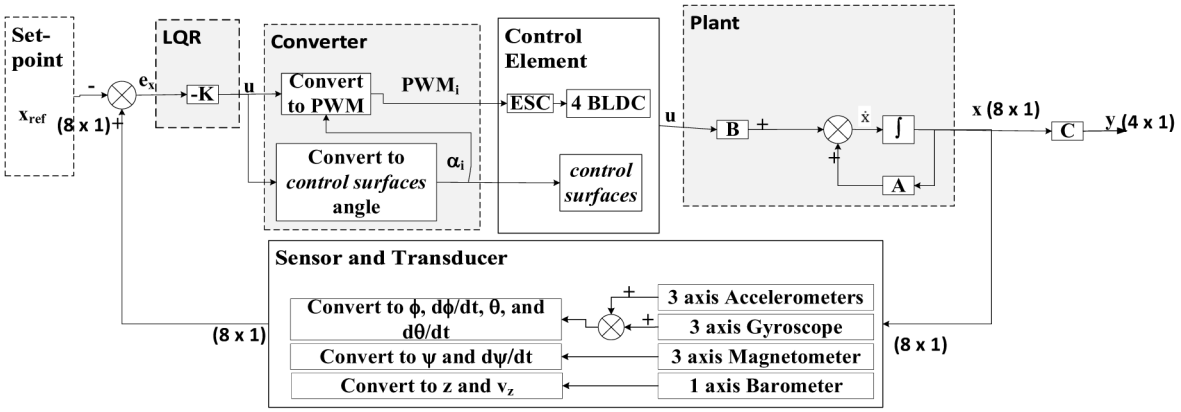

FIGURE 2. Block diagram of the control system for hovering QTW UAV

4. **Results and Discussions.** The control system model is simulated using the parameters of the UAV in the real world. The simulation was carried out by tuning the matrix **Q** and **R** values from the LQR method [22]. Tuning is done in several steps using an application designed with the above parameters adjusted automatically. LQR helps in computing an initial reference value that will be enforced across the system widely.

The component values of the **Q** matrix consist of Q_z (Q vertical movement on the z-axis), Q_{v_z} (Q vertical velocity on the z-axis), Q_ϕ (Q roll angle), Q_θ (Q pitch angle), Q_ψ (Q yaw angle), $Q_{\dot{\phi}}$ (Q roll angular velocity), $Q_{\dot{\theta}}$ (Q pitch angular velocity), and $Q_{\dot{\psi}}$ (Q yaw angle velocity). Full state feedback gain **K** is the result that emerges from the LQR tuning process.

The control stabilization against roll motion disturbances on the QTW UAV (roll angle, pitch, and yaw) begins by determining the values of Q_ϕ, $Q_{\dot{\phi}}$, $Q_{\dot{\theta}}$, Q_θ, Q_ψ, and $Q_{\dot{\psi}}$. The tuning results are used to generate values for $K_{\phi\cdot\tau_\phi}$, $K_{\dot{\phi}\cdot\tau_\phi}$, $K_{\theta\cdot\tau_\theta}$, $K_{\dot{\theta}\cdot\tau_\theta}$, $K_{\psi\cdot\tau_\psi}$, and $K_{\dot{\psi}\cdot\tau_\psi}$. The higher the **Q** value, the faster the system response because of better torque values τ_ϕ, τ_θ, and τ_ψ. However, if the value of Q_ϕ, $Q_{\dot{\phi}}$, $Q_{\dot{\theta}}$, Q_θ, Q_ψ and $Q_{\dot{\psi}}$ is too large, it can cause τ_ϕ, τ_θ, and τ_ψ to increase in such a way that the system becomes very sensitive to disturbance. The values of the tuning components Q_ϕ, $Q_{\dot{\phi}}$, $Q_{\dot{\theta}}$, Q_θ, Q_ψ and $Q_{\dot{\psi}}$ can be seen in Table 1.

TABLE 1. Optimal **Q** and **K** values for attitude control QTW UAV

Q	**R**	**K**
$Q_\phi = 2500$	$R_\phi = 1$	$K_{\phi\cdot\tau_\phi} = 50$
$Q_{\dot{\phi}} = 20$	$R_{\dot{\phi}} = 1$	$K_{\dot{\phi}\cdot\tau_\phi} = 7.77817459$
$Q_\theta = 2500$	$R_\theta = 1$	$K_{\theta\cdot\tau_\theta} = 50$
$Q_{\dot{\theta}} = 20$	$R_{\dot{\theta}} = 1$	$K_{\dot{\theta}\cdot\tau_\theta} = 7.77817459$
$Q_\psi = 1800$	$R_\psi = 1$	$K_{\psi\cdot\tau_\psi} = 42.42640687$
$Q_{\dot{\psi}} = 30$	$R_{\dot{\psi}} = 1$	$K_{\dot{\psi}\cdot\tau_\psi} = 9.54431904$

Tests were carried out on roll, pitch, and yaw rotations. The test has been carried out by providing disturbances at the ϕ, θ, and ψ angles of 10°. The test results are conducted by observing how fast the system response gives an error response of 0. The test results can be seen in Figure 3 which shows that the roll ϕ and pitch θ angle response speeds are faster than that of the yaw ψ. The control system can overcome the error response on roll and pitch angles within 0.4 seconds, and that on the yaw angle, 0.6 seconds.

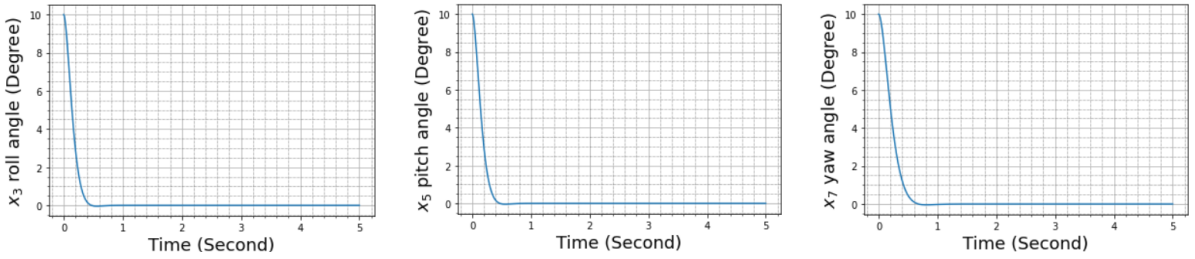

(a) (b) (c)

FIGURE 3. Responses to errors in rotational motion against time with an error of 10°: (a) Roll ϕ; (b) Pitch θ; (c) Yaw ψ

The second test was carried out by providing disturbances at ϕ, θ, and ψ angles of 30°. The test results can be seen in Figure 4. In Figure 4, the response speeds of the roll and pitch angles are faster than that of the yaw angle. The control system can overcome error responses on roll and pitch angles within 0.5 seconds, and that of the yaw angle, 0.65 seconds.

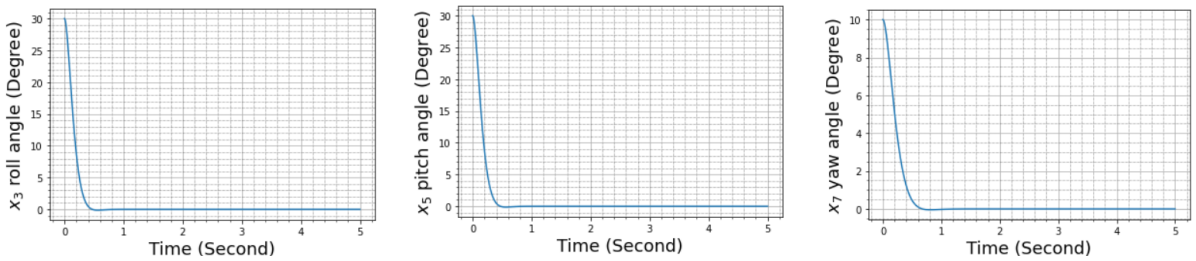

(a) (b) (c)

FIGURE 4. Responses to errors in rotational motion against time with an error of 30°: (a) Roll ϕ; (b) Pitch θ; (c) Yaw ψ

Altitude control on the QTW UAV (vertical axis in the Earth's inertial frame) begins by determining the component values Q_z and Q_{v_z}. The tuning results of the Q_z and Q_{v_z} values are used to control the UAV's QTW altitude close to stationary so that the error response is close to zero. In the simulation, a one-meter error is introduced on the z-axis. The process of tuning the values of Q_z and Q_{v_z} produces gains $K_{z \cdot F_z}$ and $K_{v_z \cdot F_z}$. The higher the **Q** value, the faster the response because the F_z value is rising. However, if the value of Q_z and Q_{v_z} is too large, it can cause F_z to increase the system becoming susceptible to disturbances. The values of the tuning components Q_z and Q_{v_z} can be seen in Table 2.

TABLE 2. Optimal **Q** and **K** values for altitude control QTW UAV

Q	**R**	**K**
$Q_z = 900$	$R_z = 1$	$K_{z \cdot F_z} = 30$
$Q_{v_z} = 30$	$R_{v_z} = 1$	$K_{v_z \cdot F_z} = 17.32050808$

The test was carried out on the vertical motion on the z-axis. Testing was done by providing interference on the z-axis. The test results showed how fast the system response is to return the error response to 0. The test was carried out by providing a disturbance on the z-axis of 1 meter. The test results can be seen in Figure 5.

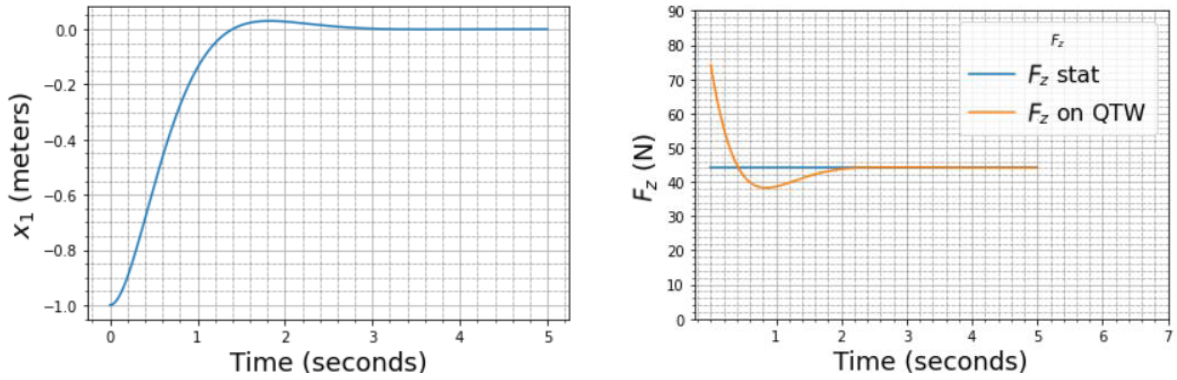

(a) (b)

FIGURE 5. Error responses on the z-axis: (a) Height adjustment response; (b) Magnitude of force required to produce the response

When the QTW UAV is in hover mode, it can be seen from Figure 5 that the QTW UAV can correct the altitude with an error of 1 meter in 1.2 seconds. The total lift generated by the four motors is around 74 N.

5. **Conclusions.** Based on the simulation results, it can be concluded that the QTW UAV can maintain a stationary state using the LQR method. This conclusion is indicated by the translational and rotational motion error response results. The errors are minimized close to 0 when the disturbance is given. QTW UAV can improve altitude and overcome error responses in roll, pitch, and yaw angles according to the desired results. The results show that the control system on the QTW UAV can be appropriately controlled.

Work is undergoing to simulate the control when the QTW UAV makes a transition flight from hover mode to cruise flight mode.

Acknowledgment. Ministry of Education, Culture, Research, and Technology, Republic of Indonesia supported this work under the BPPDN scholarship 2019.

REFERENCES

[1] E. Euteneuer and G. Papageorgiou, UAS insertion into commercial airspace: Europe and US standards perspective, *IEEE/AIAA 30th Digital Avionics Systems Conference*, DOI: 10.1109/DASC.2011.6096249, 2011.

[2] G. Nugroho, A. Dharmawan, D. Lelono and A. M. Handayani, Waypoint tracking of a fixed-wing UAV using the L1 cross track error control, *ICIC Express Letters, Part B: Applications*, vol.13, no.2, pp.115-122, DOI: 10.24507/icicelb.13.02.115, 2022.

[3] T. Mikami and K. Uchiyana, Design of flight control system for quad tilt-wing UAV, *2015 International Conference on Unmanned Aircraft Systems (ICUAS)*, pp.801-805, DOI: 10.1109/ICUAS.2015.7152364, 2015.

[4] A. Dharmawan, A. Ashari, A. G. Aprilia and A. M. Handayani, Auto VTOL system on quadrotor using Madgwick quaternion Kalman filter and LQR, *2018 4th International Conference on Science and Technology (ICST)*, vol.1, pp.1-6, DOI: 10.1109/ICSTC.2018.8528613, 2018.

[5] D. Matouk, F. Abdessemed, O. Gherouat and Y. Terchi, Second-order sliding mode for position and attitude tracking control of quadcopter UAV: Super-twisting algorithm, *International Journal of Innovative Computing, Information and Control*, vol.16, no.1, pp.29-43, DOI: 10.24507/ijicic.16.01.29, 2020.

[6] S. Suzuki et al., Attitude control of quad rotors QTW-UAV with tilt wing mechanism, *Journal of System Design and Dynamics*, vol.4, no.3, pp.416-428, DOI: 10.1299/jsdd.4.416, 2010.
[7] H. Gu, X. Lyu, Z. Li, S. Shen and F. Zhang, Development and experimental verification of a hybrid vertical take-off and landing (VTOL) unmanned aerial vehicle (UAV), *2017 International Conference on Unmanned Aircraft Systems (ICUAS)*, pp.160-169, DOI: 10.1109/ ICUAS.2017.7991420, 2017.
[8] S. Panza, M. Sato, M. Lovera and K. Muraoka, Robust attitude control design of quad-tilt-wing UAV: A structured μ-synthesis approach, *2018 IEEE Conference on Control Technology and Applications*, pp.781-786, DOI: 10.1109/CCTA.2018.8511407, 2018.
[9] L. M. Sanchez-Rivera, R. Lozano and A. Arias-Montano, Development, modeling and control of a dual tilt-wing UAV in vertical flight, *Drones*, vol.4, no.4, pp.1-15, DOI: 10.3390/drones4040071, 2020.
[10] K. Nonami, F. Kendoul, S. Suzuki, W. Wang and D. Nakazawa, *Autonomous Flying Robots*, Springer, Tokyo, Japan, 2010.
[11] E. Small, E. Fresk, G. Andrikopoulos and G. Nikolakopoulos, Modelling and control of a tilt-wing unmanned aerial vehicle, *2016 24th Mediterranean Conference on Control and Automation (MED)*, pp.1254-1259, DOI: 10.1109/MED.2016.7536050, 2016.
[12] M. Sato and K. Muraoka, Flight control of quad tilt wing unmanned aerial vehicle, *The Japan Society for Aeronautical and Space Sciences*, vol.61, no.4, pp.110-118, DOI: 10.2322/jjsass.61.110, 2013.
[13] M. Sato, K. Muraoka and E. Agency, Flight controller design and demonstration of quad-tilt-wing unmanned aerial vehicle, *Journal of Guidance, Control, and Dynamics*, vol.38, no.6, pp.1-12, DOI: 10.2514/1.G000263, 2015.
[14] A. Dharmawan, L. Ichsan, H. Baskoro, J. E. Istiyanto and A. M. Handayani, Attitude and horizontal speed control system on unmanned aerial vehicle using LQR, *2019 5th International Conference on Science and Technology (ICST)*, pp.1-6, DOI: 10.1109/ICST47872. 2019.9166192, 2019.
[15] K. Benkhoud and S. Bouallegue, Modeling and LQG controller design for a quad tilt-wing UAV, *The 3rd International Conference on Automation, Control Engineering and Computer Science (ACECS); Proceedings of Engineering and Technology (PET)*, vol.13, pp.198-204, 2016.
[16] K. B. Khoud, S. Bouallègue and M. Ayadi, Design and co-simulation of a fuzzy gain-scheduled PID controller based on particle swarm optimization algorithms for a quad tilt wing unmanned aerial vehicle, *Transactions of the Institute of Measurement and Control*, vol.40, no.14, pp.3933-3952, DOI: 10.1177/0142331217740947, 2018.
[17] C. Hancer, K. T. Oner, E. Sirimoglu, E. Cetinsoy and M. Unel, Robust hovering control of a quad tilt-wing UAV, *IECON 2010 – The 36th Annual Conference on IEEE Industrial Electronics Society*, pp.1615-1620, DOI: 10.1109/IECON.2010.5675441, 2010.
[18] Y. Yildiz, M. Unel and A. E. Demirel, Nonlinear hierarchical control of a quad tilt-wing UAV: An adaptive control approach, *International Journal of Adaptive Control and Signal Processing*, vol.31, no.9, pp.1245-1264, DOI: 10.1002/acs.2759, 2017.
[19] Y. Yildiz, M. Unel and A. E. Demirel, Adaptive nonlinear hierarchical control of a quad tilt-wing UAV, *2015 European Control Conference (ECC)*, DOI: 10.1109/ECC.2015.7331093, 2015.
[20] A. Ashari and A. Dharmawan, Altitude and flight speed control system on vtol-plane UAVs using the LQR method, *ICIC Express Letters, Part B: Applications*, vol.13, no.3, pp.225-232, DOI: 10.24507/icicelb.13.03.225, 2022.
[21] K. Ogata, *Modern Control Engineering*, 5th Edition, Prentice-Hall, New Jersey, USA, 2010.
[22] F. Rinaldi, S. Chiesa and F. Quagliotti, Linear quadratic control for quadrotors UAVs dynamics and formation flight, *Journal of Intelligent and Robotic Systems*, vol.70, nos.1-4, pp.203-220, DOI: 10.1007/s10846-012-9708-3, 2012.